TRAC-M-TR-19-023
June 2019

Estimating Geometric Intervisibility to the Aerial Layer with Military Applications

The Research and Analysis Center
700 Dyer Road
Monterey, CA 93943-0692

This study cost the Department of Defense approximately $63,000 expended by TRAC in Fiscal Years 18-19.
Prepared on 20190619
TRAC Project Code # 060332

THIS PAGE INTENTIONALLY LEFT BLANK

TRAC-M-TR-19-020
MAY 2019

Estimating Geometric Intervisibility to the Aerial Layer with Military Applications

Authors

MAJ James Jablonski
Dr. Jonathan Alt

PREPARED BY:

MAJ James Jablonski
MAJ, US Army
TRAC-MTRY

APPROVED BY:

LTC Brian Wade
LTC, US Army
Director, TRAC-MTRY

THIS PAGE INTENTIONALLY LEFT BLANK

REPORT DOCUMENTATION PAGE			*Form Approved OMB No. 0704-0188*
Public reporting burden for this collection of information is estimated to average 1 hour per response, including the time for reviewing instruction, searching existing data sources, gathering and maintaining the data needed, and completing and reviewing the collection of information. Send comments regarding this burden estimate or any other aspect of this collection of information, including suggestions for reducing this burden, to Washington headquarters Services, Directorate for Information Operations and Reports, 1215 Jefferson Davis Highway, Suite 1204, Arlington, VA 22202-4302, and to the Office of Management and Budget, Paperwork Reduction Project (0704-0188) Washington DC 20503.			
1. AGENCY USE ONLY ***(Leave blank)***	**2. REPORT DATE** 19 June 2019	**3. REPORT TYPE AND DATES COVERED** Technical Report, November 2017 to June 2019	
4. TITLE AND SUBTITLE Estimating Geometric Intervisibility to the Aerial Layer with Military Applications			**5. PROJECT NUMBERS** TRAC Project Code 060332
6. AUTHOR(S) MAJ James Jablonski, Dr. Jonathan Alt			
7. PERFORMING ORGANIZATION NAME(S) AND ADDRESS(ES) US Army The Research and Analysis Center - Monterey 700 Dyer Road Monterey CA, 93943-0692			**8. PERFORMING ORGANIZATION REPORT NUMBER** TRAC-M-TR-19-023
9. SPONSORING /MONITORING AGENCY NAME(S) AND ADDRESS(ES) HQDA G-8 FD			**10. SPONSORING/MONITORING AGENCY REPORT NUMBER** n/a
11. SUPPLEMENTARY NOTES Findings of this report are not to be construed as an official Department of the Army (DA) position unless so designated by other authorized documents.			
12a. DISTRIBUTION / AVAILABILITY STATEMENT Approved for public release; distribution is unlimited			**12b. DISTRIBUTION CODE**

13. ABSTRACT (maximum 200 words)

Terrain affects air maneuver and defense by creating covered and concealed routes based on the geometry of an area. Tactical flight and air defense planning both depend on understanding terrain and the associated effects of altitude, airspeed, and potential countermeasures. This research developed methods to characterize the level of exposure throughout the aerial layer in a given terrain and derived two exposure metrics from geometric intervisibility calculations conducted at scale. We compare the information provided by each metric along with the computational costs for a given terrain size. This research developed a methodology to characterize the level of exposure in a given terrain and demonstrates proof of principle application of the developed data to inform routing and site selection problems encountered by military planners. Methods exist to characterize the exposure to ground visibility along a user-defined route at a single altitude, but methods to characterize the level of exposure for an entire terrain box are not readily available.

14. SUBJECT TERMS Aerial exposure, terrain, visibility analysis			**15. NUMBER OF PAGES** 27
			16. PRICE CODE
17. SECURITY CLASSIFICATION OF REPORT Unclassified	**18. SECURITY CLASSIFICATION OF THIS PAGE** Unclassified	**19. SECURITY CLASSIFICATION OF ABSTRACT** Unclassified	**20. LIMITATION OF ABSTRACT** UU

NSN 7540-01-280-5500

Standard Form 298 (Rev. 2-89)
Prescribed by ANSI Std. 239-18

THIS PAGE INTENTIONALLY LEFT BLANK

NOTICES

DISCLAIMER

Findings of this report are not to be construed as an official Department of the Army (DA) position unless so designated by other authorized documents.

REPRODUCTION

DISTRIBUTION STATEMENT

Approved for public release; distribution is unlimited.

DESTRUCTION NOTICE

When this report is no longer needed, DA organizations will destroy it according to procedures given in AR 380-5, DA Information Security Program. All others will return this report to Director, TRAC, ATTN: ATRC, 255 Sedgwick Avenue, Fort Leavenworth, Kansas 66027-2345.

THIS PAGE INTENTIONALLY LEFT BLANK

ABSTRACT

Terrain affects air maneuver and defense by creating covered and concealed routes based on the geometry of an area. Tactical flight and air defense planning both depend on understanding terrain and the associated effects of altitude, airspeed, and potential countermeasures. This research developed methods to characterize the level of exposure throughout the aerial layer in a given terrain and derived two exposure metrics from geometric intervisibility calculations conducted at scale. We compare the information provided by each metric along with the computational costs for a given terrain size. This research developed a methodology to characterize the level of exposure in a given terrain and demonstrates proof of principle application of the developed data to inform routing and site selection problems encountered by military planners. Methods exist to characterize the exposure to ground visibility along a user-defined route at a single altitude, but methods to characterize the level of exposure for an entire terrain box are not readily available.

THIS PAGE INTENTIONALLY LEFT BLANK

TABLE OF CONTENTS

LIST OF FIGURES

THIS PAGE INTENTIONALLY LEFT BLANK

LIST OF TABLES

LIST OF ACRONYMS AND ABBREVIATIONS

ADA: Air Defense Artillery

DTED: Digital Terrain Elevation Data

DEM: Digital Elevation Model

FVL: Future Vertical Lift

GIS: Geographic Information System

HPC: High Performance Computing

NPS: Naval Postgraduate School

TRAC: The Research and Analysis Center

THIS PAGE INTENTIONALLY LEFT BLANK

ACKNOWLEDGMENTS

I would like to thank TRAC for the opportunity to conduct this important research and NPS for the use of their high-performance computing assets that made it possible.

THIS PAGE INTENTIONALLY LEFT BLANK

INTRODUCTION

1.1. PURPOSE

Route planning for military air operations requires an understanding of the terrain and threat, along with consideration of altitude, airspeed, and friendly countermeasures. Air defense site selection requires consideration of similar factors. While tools exist to facilitate this process, they largely rely on human subject matter expertise to identify covered and concealed routes [1]. A priori planning can then be validated by determining the level of exposure to ground line of site along the specified route, but no current tools suggest alternative routings with lower exposure levels. Likewise, tools exist to determine the amount of airspace covered by a set of air defense assets, but they do not provide a recommended set of locations to maximize coverage of a given avenue of approach. Planning of all military operations begins with a detailed terrain analysis -- this research develops methods to facilitate data driven analysis of the effects of terrain on aerial maneuver and defensive operations [1].

1.2. PROJECT SUMMARY

We first develop methods to characterize the level of exposure throughout the aerial layer in a given terrain box, where two exposure metrics are derived from geometric inter visibility calculations conducted at scale. We compare the information provided by each metric along with the computational costs for a given terrain box. We then demonstrate the use of these metrics to inform a routing algorithm that minimizes exposure at a given altitude and to inform the selection of air defense sites that maximize coverage along a given avenue of approach. Finally, we summarize the results of this research and discuss directions for future work.

1.3. BACKGROUND

The impact of terrain on terrestrial military operations is well documented and studied. Military planners conduct an analysis of the impact of terrain on their operations as a routine step in the planning process [2]. Geographic information systems (GIS) support this planning process by facilitating objective data-driven analysis in a timely manner for many use cases. Determining the level of intervisibility between locations in the terrestrial layer is of prime concern to many

military applications, and much focus has been placed on creating methods to efficiently conduct these calculations for limited numbers of locations in a terrain box. Tools to facilitate the same type of objective analysis for aerial route planning exist, but are limited to the examination of points along defined routes. With relatively recent advances in access to computational assets and the ability store and provision data for re-use, many potential applications might now be enabled by data produced from these relatively simple calculations conducted at scale and packaged for re-use.

The GIS community studies the problem of determining line of sight between two points on the ground, and the most closely related concepts from this field are the viewshed and skyview. A viewshed describes all the points in a given terrain box that are visible from a given location within the box. A skyview by contrast determines the fraction of the sky visible from a given location on the ground. The standard implementations of these concepts look at only single points rather than an entire piece of terrain [3].

Existing algorithms used in both modern GIS such as GRASS and ARC-GIS typically consider only the viewshed of a single point at a given observation elevation for both target and viewpoint [4] [5] [6]. Using this approach to determine the intervisiblity between all points on the ground and all altitudes in the aerial layer would require iterations at multiple altitudes for each point on the ground, resulting in $O(n^2a)$ computational costs where a represents the number of levels in the aerial layer that require exploration.

The total-viewshed provides information about intervisibility between all points in a terrain box. Tabik et. al. demonstrate methods to simultaneously speed up the calculation of the total viewshed for a given terrain box by efficiently sampling subareas and maximizing the reutilization of computations [5]. This highly efficient method remains limited by computing the viewshed at a single height above the viewpoint.

In the next section, we develop two aerial exposure metrics based on intervisibility and describe their computation.

1.4. CONSTRAINTS, LIMITATIONS, & ASSUMPTIONS

Constraints:

- Project completion by June 2019.

Limitations:

- Data storage on NPS HPS available to conduct this study is ~100 TB.
- Exposure initially only considers geometric intra-visibility (no considerations of physics of light, etc.).

Assumptions:

- Geometric intervisibility is sufficient to inform exposure metric without considerations of other features such as trees, buildings, or potential weather conditions.
- Transition partners have access to similar architecture to enable use of the output data.
- Terrain in initial test case (DTED Level 2 9KM x 27KM eastern European) is sufficient to understand the computational and storage costs and inform efforts to scale the approach.

1.5. STUDY TEAM

MAJ James Jablonski

Dr. Jonathan Alt

THIS PAGE INTENTIONALLY LEFT BLANK

SECTION 2. METHODOLOGY

2.1. INTERVISIBILITY CALCULATION

The calculation of the exposure metrics presented here relies on the total viewshed for the full aerial layer. This requires calculating the inter visibility between each point in the terrestrial layer and all points in the sky over a terrain box. In order to facilitate the use of these metrics on realistic terrain boxes, we first explore methods to efficiently conduct this calculation.

The standard viewshed algorithm proceeds by determining, for each target location or cell in a grid, whether a line segment drawn from the viewpoint to the target intersects cells in the terrain. If terrain is intersected, the target location is not visible. This is determined by calculating the gradient from the viewpoint to the target pixel and comparing this to the gradient of all locations between. This methodology requires $O(n^2 a)$ tests with n pixels and a elevations. GIS systems leverage a radial sweep method to organize the calculations and reduce the overhead of sorting and memory reads and writes [4].

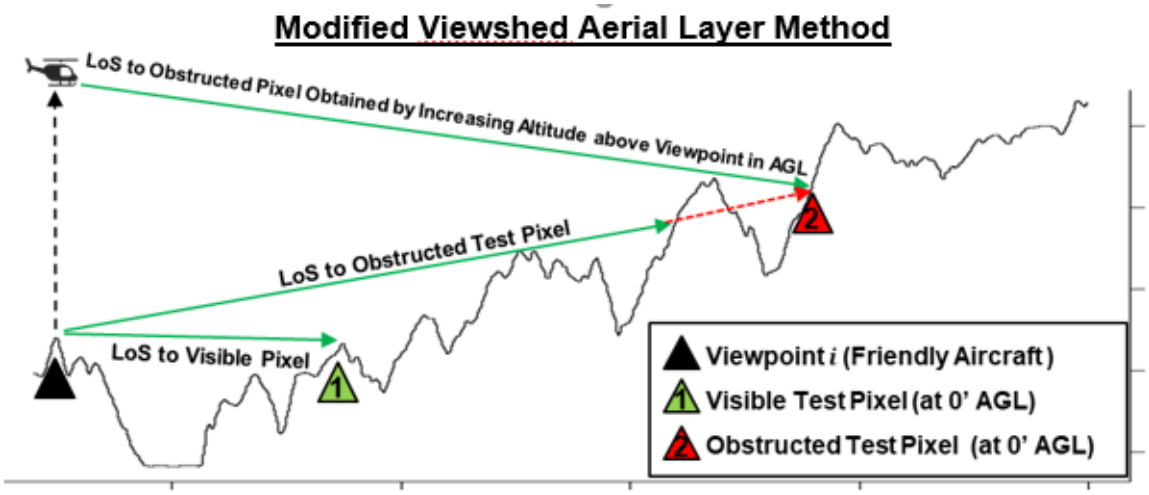

Figure 1: Modified Viewshed Algorithm

We modify the standard viewshed algorithm by calculating the viewpoint altitude required to achieve intervisibility to the target, as illustrated by Figure 1. This results in a single numeric matrix for each viewpoint. The matrix represents target locations that are visible from the veiwpoint at the surface of the terrain with a zero. Locations not visible from the surface are stored as positive values indicating the altitude required to 'see' the target pixel from the viewpoint. To accomplish this, we calculate the veiwpoint altitude required for all pixels between the target and

viewpoint and select the maximum result. As with most other viewshed implementations, the calculations are organized for efficiency using a radial sweep method. To provide clarity, pseudocode for the algorithm is provided in figure Figure 2. The aerial intervisibility matrix is then stored in a visibility array where all locations correspond to a modified viewshed result.

Pseudocode:

For a terrain with matrix of I elevation measurements.
for i *in* I as Viewpoints
  for i *in* I *as Test Pixels*
    if *gradient* ∇ *to Test Pixel* $I > \nabla$ *to all pixels between Test and Viewpoint*
      then Pixel is *Visible*, ***record result*** $\boldsymbol{VIS_{i,i}}$ ***as*** $\mathbf{0}$
    else - *Test Pixel is not Visible*
      Record result $\boldsymbol{VIS_{i,i}}$ ***as elevation (AGL) required for*** ∇ ***to be > all pixels between test & Viewpoint.***

Figure 2: Modified Viewshed Algorithm Pseudocode

The methodology requires $O(n^2)$ tests with n pixels to solve for all viewpoint elevations simultaneously. The computational cost for each individual test increases when compared to other methods, but ultimately provides storage and computational savings. In use cases where more than just one or a few altitudes are required, the modified viewshed results in significantly less storage requirements. When applications permit, further efficiency can be gained by limiting the distance considered by the algorithm.

When comparing our approach to common GIS systems, we note some key differences. ArcGIS, a commonly used and longstanding GIS platform, offers both viewshed and visibility calculations, but does not provide for calculation of the total-viewshed [7]. The data can be calculated by calculating the viewshied at all points in the map as in, or by using the visibility tool [8]. To use this approach for the aerial layer, the process would then have to be repeated for multiple altitudes based on the desired aerial resolution. GRASS GIS, a powerful open source platform, does not offer an aerial visibility specific tool, but can record the difference between the observer and target pixel's elevation as an output raster during viewshed calculations [9].

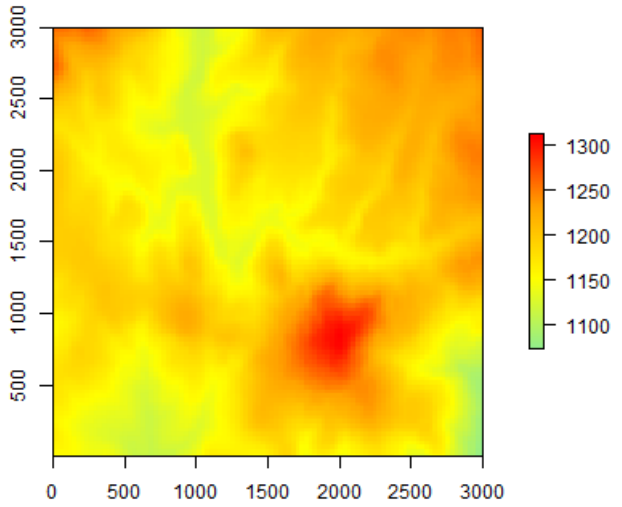

Figure 3: Randomly selected European terrain. 30M resolution digittal elevation model.

For the initial proof of principle implementation, the 3KM x 3KM, 30m resolution digital elevation model shown in Figure 3 was used and run on an Intel(R) Core i7-7600U Windows laptop with 16 GB of RAM. The associated exposure metric calculations were then calculated on the same laptop, and required minimal additional processing due to the pre-calculation of the visibility array. In order to scale the intervisibility calculations up to a more realistic terrain box, the team made use of high performance computing assets available at the Naval Postgraduate School. The calculations for the greater than 500K points in the 9KM x 27KM terrain box were parallelized in this environment, running on 500 nodes, and producing approximately a third of a terrabyte of output data.

2.2. EXPOSURE METRIC

This section presents two formulations of the exposure metric produced from the aerial intervisibility calculations described above. Naive exposure represents total exposure to visibility from the ground at a given elevation, while windowed exposure considers susceptibility to engagement at a given speed and elevation. The formulations are presented below, with sample exposure metric scores for the 3x3 km DEM presented in Figure 3.

3.5.2 NAÏVE EXPOSURE

We define a naive exposure metric as the ratio of locations on the ground, within a given range, that are visible from a point at a set altitude. The formulation is provided in equation

Equation 1. Our methodology leverages the pre-calculated intervisibility array generated by the modified viewshed algorithm to calculate exposure. This approach enables the timely calculation of exposure at different altitudes

Where:

$i \in I$ *locations in a digital elevation model.*

$p \in P$ *locations within range to point* i.

a *is a given altitude.*

$VIS_{p,a}$ *is binary,* 1 *if pointi is visible at altitude* a, 0 *otherwise.*

$$exposure(i) = \frac{\sum_{\forall p \in P} VIS_{p,a}}{|p|}$$

Equation 1

We modify the standard viewshed algorithm by calculating the viewpoint altitude required to achieve intervisibility to the target, as illustrated by Figure 1. This results in a single numeric matrix for each viewpoint. The matrix represents target locations that are visible from the veiwpoint at the surface of the terrain with a zero. Locations not visible from the surface are stored as positive values indicating the altitude required to 'see' the target pixel from the viewpoint. To accomplish this, we calculate the viewpoint altitude required for all pixels between the target and viewpoint and select the maximum result. As with most other viewshed implementations, the calculations are organized for efficiency using a radial sweep method. To provide clarity, pseudocode for the algorithm is provided in

Pseudocode:

For a terrain with matrix of I elevation measurements.
for i *in* I as Viewpoints
  for i *in* I *as Test Pixels*
    if *gradient* ∇ *to Test Pixel* $I >$ ∇ *to all pixels between Test and Viewpoint*
      then Pixel is *Visible,* ***record result*** $VIS_{i,i}$ ***as*** 0
    else - *Test Pixel is not Visible*
      Record result $VIS_{i,i}$ ***as elevation (AGL) required for*** ∇ ***to be*** $>$ ***all pixels between test & Viewpoint.***

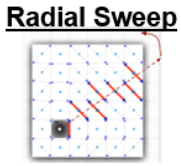

Figure 4. The aerial intervisibility matrix is then stored in a visibility array where all locations correspond to a modified viewshed result.

The methodology requires $O(n^2)$ tests with n pixels to solve for all viewpoint elevations simultaneously. The computational cost for each individual test increases when compared to other methods, but ultimately provides storage and computational savings. In use cases where more than just one or a few altitudes are required, the modified viewshed results in significantly less storage requirements. When applications permit, further efficiency can be gained by limiting the distance considered by the algorithm.

Pseudocode:

For a terrain with matrix of I elevation measurements.
for i *in* I as Viewpoints
  for i *in* I *as Test Pixels*
    if *gradient* ∇ *to Test Pixel* $I >$ ∇ *to all pixels between Test and Viewpoint*
      then Pixel is *Visible,* ***record result*** $VIS_{i,i}$ ***as*** **0**
    else - *Test Pixel is not Visible*
      Record result $VIS_{i,i}$ ***as elevation (AGL) required for*** ∇ ***to be*** $>$ ***all pixels between test & Viewpoint.***

Radial Sweep

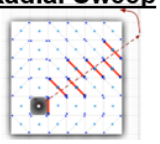

Figure 4: Modified Viewshed Algorithm Pseudocode

When comparing our approach to common GIS systems, we note some key differences. ArcGIS, a commonly used and longstanding GIS platform, offers both viewshed and visibility calculations, but does not provide for calculation of the total-viewshed [7]. The data can be calculated by calculating the viewshied at all points in the map as in, or by using the visibility tool \citep{paralell}. To use this approach for the aerial layer, the process would then have to be repeated for multiple altitudes based on the desired aerial resolution. GRASS GIS, a powerful open source platform, does not offer an aerial visibility specific tool, but can record the difference between the observer and target pixel's elevation as an output raster during viewshed calculations [9].

The results illustrated in Figure 5 are intuitive. Points located above areas where we can expect lower visibility such as canyons have lower exposure scores, with the opposite result above points of generally higher elevation in open areas or on hilltops. One can visually confirm the results of Franklin and Ray observing that higher elevation does not always correspond to higher exposure [10]. Exposure also dramatically increases with altitude, an intuitive, but important result to quantify and understand more fully.

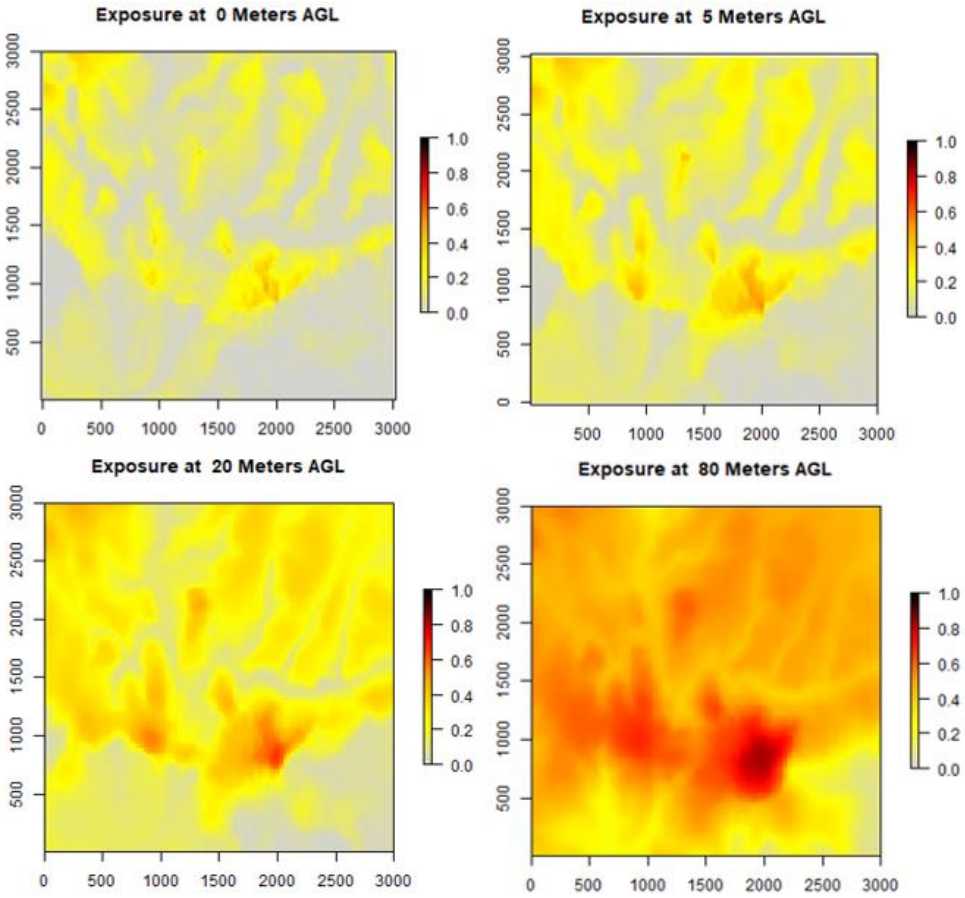

Figure 5: Naive exposure calculated on the 3x3 km DEM at increasing altitudes from left to right (0, 5, 20, and 80 meters AGL).

3.5.2 WINDOWED EXPOSURE

The second metric differs from the naive metric by incorporating the idea of exposure windows tied to the time required for a threat to engage a target. An aircraft in the sky is 'exposed' to a point on the ground if it remains visible to that point while traveling at a given speed and direction along a vector for the required threat engagement time. We define engagement time as the total time an enemy air defense system needs continuous visibility on an aircraft to complete a successful engagement. Determination of visibility along the vector requires iterative calculations of our naive metric to determine if the aerial path remains continuously visible from individual points on the ground. The formulation for our windowed metric is provided below in Equation 2.

$\underline{Where}$:

$i \in I\ locations\ in\ a\ digital\ elevation\ model.$

$p \in P\ locations\ within\ range\ to\ point\ i.$

$a\ is\ a\ given\ altitude.$

$r \in R\ directions\ of\ travel\ from\ i(0 - 360).$

$t\ is\ the\ expected\ time\ required\ for\ enemy\ aquisition\ and\ engagement.$

$v\ is\ the\ aircraft\ velocity$

and

$VIS_{r,a,v,t,p} is\ binary, 1\ if an\ aircraft\ remains\ continuously\ visible\ for\ t\ seconds\ from\ position\ p\ at\ elevation\ a, moving\ along\ the\ path\ in\ direction\ r\ at\ velocity\ v, 0\ otherwise.$

$$exposure(i) = \frac{\sum_{\forall p \in P} \sum_{\forall r \in R} VIS_{p,a,r,v,t}}{|p||r|}$$

Equation 2

The algorithm used to calculate the windowed metric is presented in Figure 6. Exposure, given aircraft velocity, altitude above ground, and required engagement time is calculated for all locations within the DEM. As with the naive metric, it relies on the precalculated visibility array. Our initial implementation of the windowed metric considers four directions North to South, East to West, SouthWest to NorthEast, and NorthWest to SouthEast. The aircraft is considered 'exposed' to a single point on the ground while moving in one direction, if it remains continuously visible for a distance calculated based on velocity and engagement time. We then add all four directions and divide by four to normalize. The final score for each location is the sum of this result for all points within range divided by the number of points within range. We gain efficiency by only determining continuous visibility to a point on the ground if the point itself is visible. This exposure score presents increased challenges for parallelization, but demands it due to far higher computational costs.

Pseudocode:

For a terrain with I locations in a digital elevation model, and the set P locations within range to each i, and aerial intervisibility array $\boldsymbol{VIS}$

record distance traveled $\boldsymbol{d}$ at velocity $\boldsymbol{v}$ for $\boldsymbol{t}$ seconds engagement time

for all $\boldsymbol{i}$ **in** I as aerial locations at altitude $\boldsymbol{a}$
  for all $\boldsymbol{p}$ **in** $\boldsymbol{P}$ *locations within range*
    if ($\boldsymbol{VIS}_{i,p} < \boldsymbol{a}$)
      for all $\boldsymbol{r}$ **in** $\boldsymbol{R}$ directions of travel considered (0-180, 45-225, 90-270, 135-315)
        if ($\boldsymbol{VIS}_{j,p} < a$) for all $\boldsymbol{j}$points in direction $\boldsymbol{r}$ within distance $\boldsymbol{d}$
          record 1 for $\boldsymbol{VISPath}_{i,p,r}$
      exposure$_i$ = sum($\boldsymbol{VISPath}_{i,p,r}$ ==1 for all $\boldsymbol{p}$ and $\boldsymbol{r}$)/(count(**r**) x count(p))

Figure 6: Windowed Exposure Pseudocode

Windowed exposure, calculated on the 3x3 km DEM at varying altitudes with a fixed airspeed of 300 knots and a 4 second engagement time is presented in Figure 7. Compared to the results of the naive metric, we see a slight reduction in exposure the windowed metric. There appears to be a minimal change in the overall shape and relation of exposure to the terrain. A more detailed analysis of the differences is presented below.

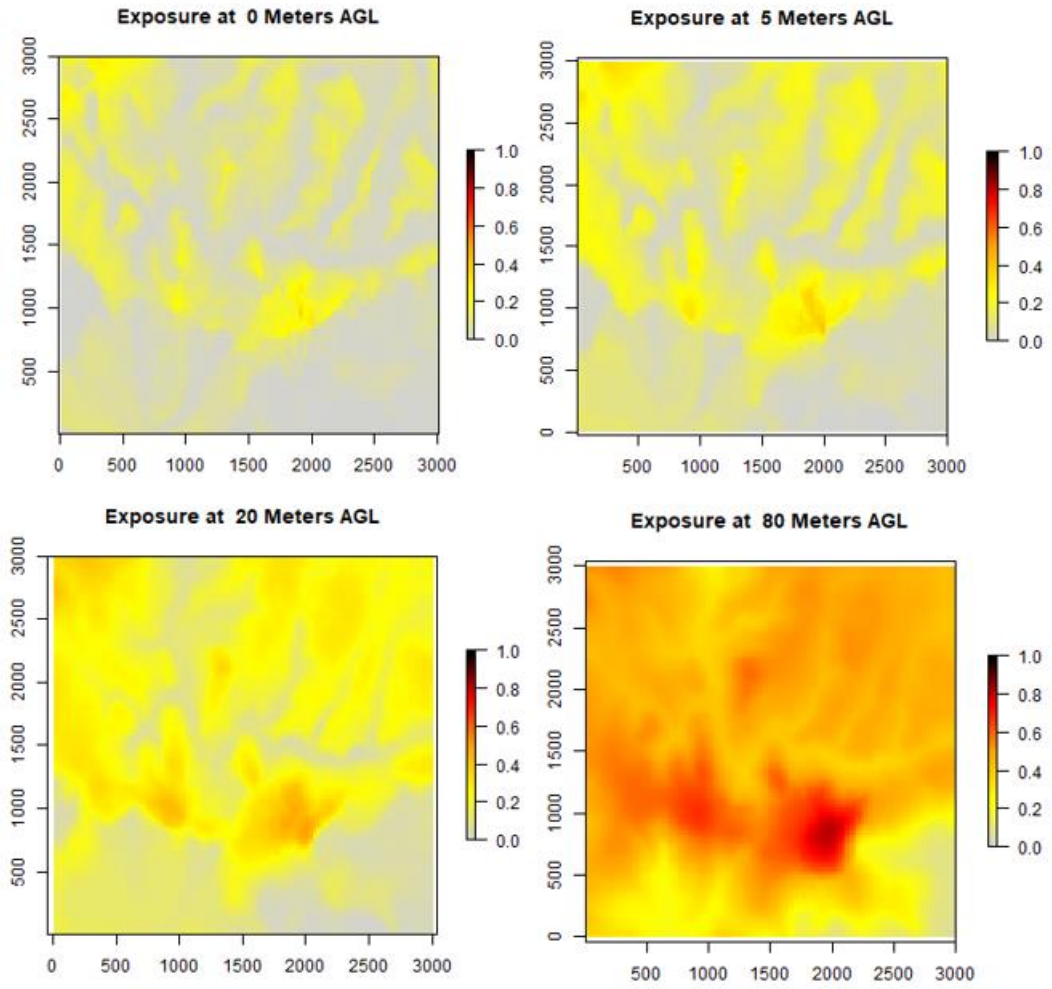

Figure 7: Windowed exposure calculated on the 3x3 km DEM, 300 knots and 4s Engagement Time at increasing altitudes from left to right (0, 5, 20, and 80 meters AGL DEM).

THIS PAGE INTENTIONALLY LEFT BLANK

SECTION 3. ANALYSIS AND FINDINGS

3.1. INTRODUCTION

This section explores differences in the two exposure scores, potential implications of exposure metric results calculated on the 3x3 km terrain, and data storage and processing time requirements. All implications drawn in this section only apply to the limited terrain analyzed, and provide the basis for future work. The storage and processing requirements section provides insight into the processing time required for determining exposure on large terrains.

3.2. EXPOSURE METRIC ANALYSIS

In order to explore the exposure metric's relationship to both the terrain and input parameters, we systematically varied all parameters for windowed and naive exposure in the 3x3 km DEM. The settings used are shown below in Table 1 where those with airspeed of zero correspond to naive exposure. We varied all parameters within operationally realistic bounds. A 2 second engagement time is unlikely for an individual air defense system, but may be possible with integrated systems. Airspeed remained within current technological bounds for rotary wing flight, and we varied altitude to correspond with terrain and contour flight levels. Some altitude and airspeed combinations may be unrealistic for current manned systems, but were included due to emerging technologies and unmanned aerial vehicles.

Altitude	Airspeed	Engagement Time
5	0	2
15	70	3
25	110	4
35	150	5
45	190	6
55	230	7
65	270	8
100		
300		

Table 1: Parameter settings for 3x3 km DEM.

The chart below in Figure 8 depicts the results of our experiment. The mean exposure across all locations within the 3x3 km DEM is plotted against airspeed, altitude, and engagement time. Upon observation, the most significant factor affecting exposure is aircraft altitude. Exposure is also dependent upon both airspeed and engagement time, which interact as expected due to the Metric 2 formulation.

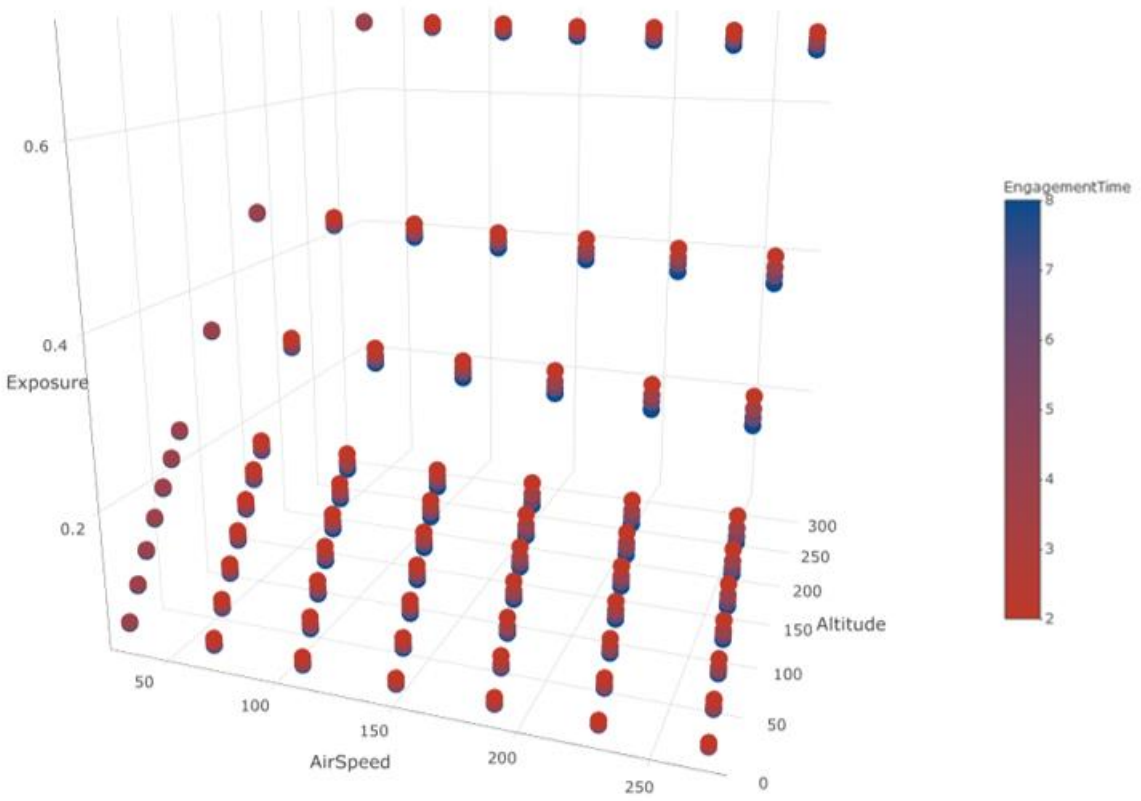

Figure 8: Three-dimensional scatterplot depicting the relationship between: 1-exposure, on the vertical axis, 2-airspeed and altitude, on the horizontal axes, and 3. engagement time, represented by marker color.

Relative to the magnitude of mean exposure, airspeed and altitude are far more influential at lower altitudes. We observe this in Figure 9. The limited size of the terrain studied may further exaggerate this issue as more distant points on the ground are more likely to be occluded by intersecting terrain. Nonetheless, the current effect appears very minimal. For example, increasing airspeed from 110 to 270 knots at a 4 second engagement time only decreases our windowed metric by 0.019 on average for the terrain. The small magnitude of exposure reduction may nonetheless prove to be operationally meaningful.

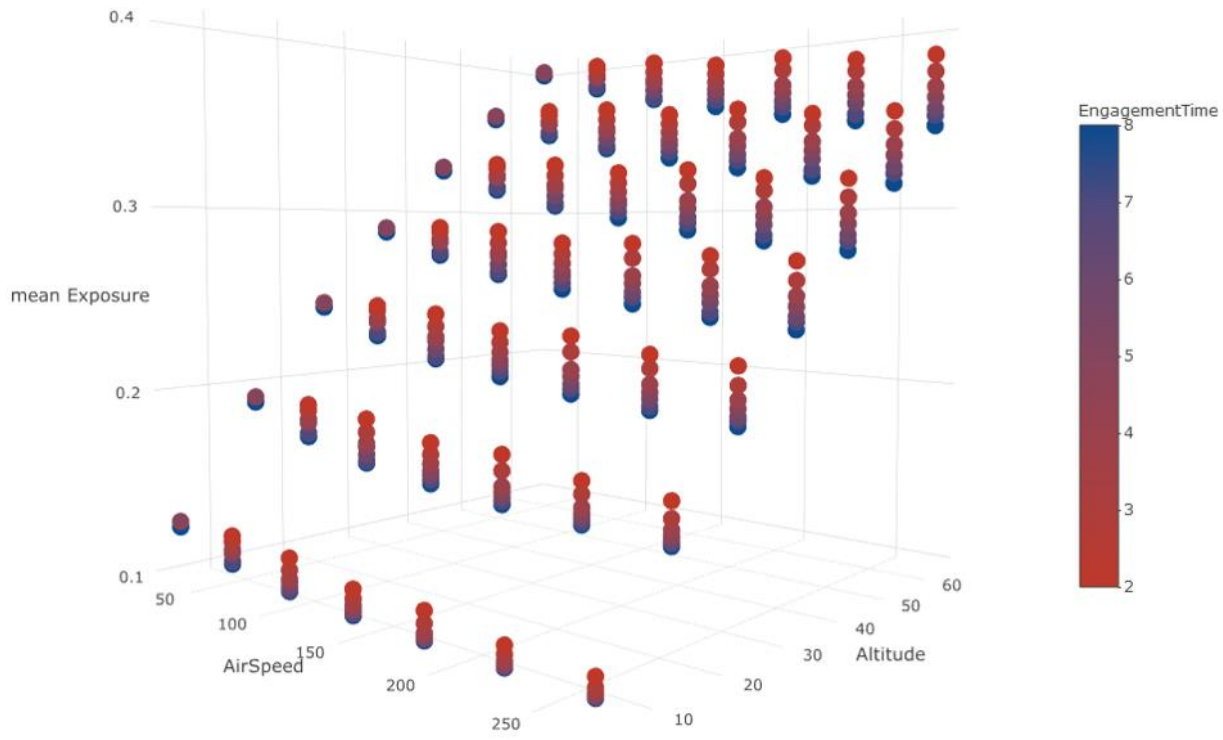

Figure 9: Three-dimensional scatterplot depicting the relationship between: 1-exposure, on the vertical axis, 2-airspeed and altitude, on the horizontal axes, and 3. engagement time, represented by marker color. This view is focused on lower altitudes to highlight

Average exposure across the entire 3x3 km DEM does not tell the entire story. Referencing figure Figure 10 we see that the complex relationship between exposure and the terrain. Close observation also reveals some differences in the overall shape between naive and windowed metrics at this altitude.

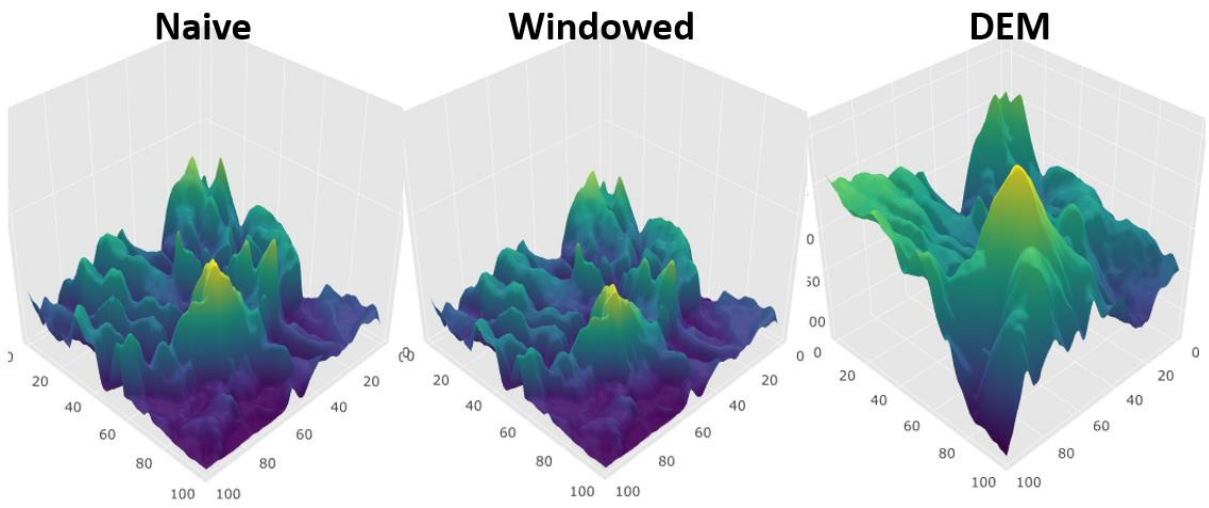

Figure 10: The three surfaces depict the naive & windowed metrics at 270 knots and 5m AGL with a 4 second engagement time. The DEM is provided for reference.

Although there are differences in the two measures, their magnitude may not be operationally meaningful enough to warrant the computational costs associated with the windowed metric, particularly for very large terrains. To explore this possibility, we examined the relationship between the two measures by constructing linear regression models. Both models used the windowed metric as the dependent variable at 300 knots airspeed and 4s engagement time, with naive exposure as the only independent variable.

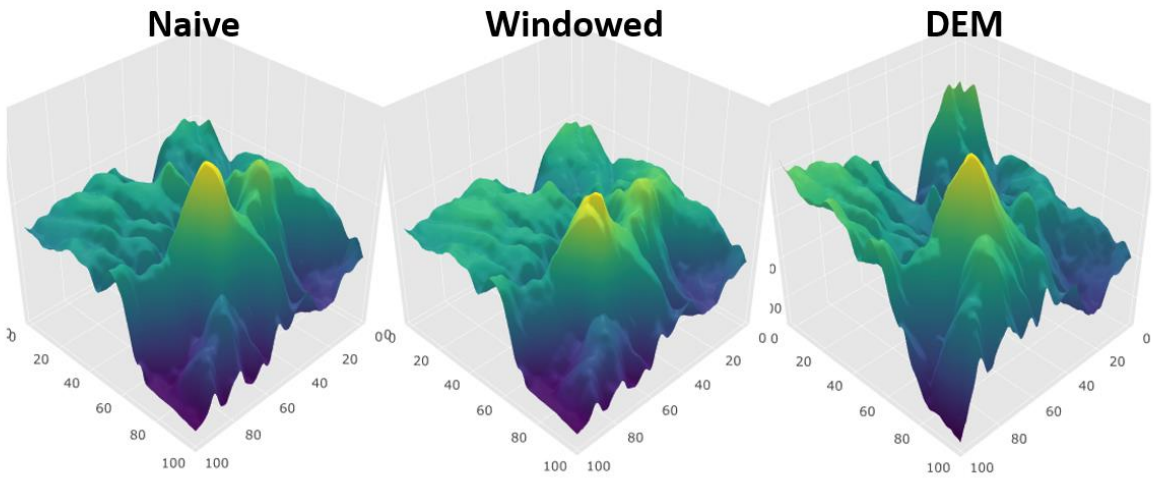

Figure 11: The three surfaces depict the naive & windowed metrics at 270 knots and 65m AGL with a 4 second engagement time. The DEM is provided for reference.

The first was run at 5m AGL, and the second at 100m and the resultant r-squared values were 0.9923 and 0.9752 respectively. Upon examining their residual plots, shown in Figure 13 we note heteroscedasticity in both. Higher variability is associated with higher exposure values, and is the result of more variability at higher altitudes in the windowed measure. Rays are more likely to be unmasked from continuous concealment when traversing over mid to high elevations. The bottom two plots in Figure 12 show the difference in magnitude between the exposure metrics, confirming the larger differences between the two measures at higher elevations.

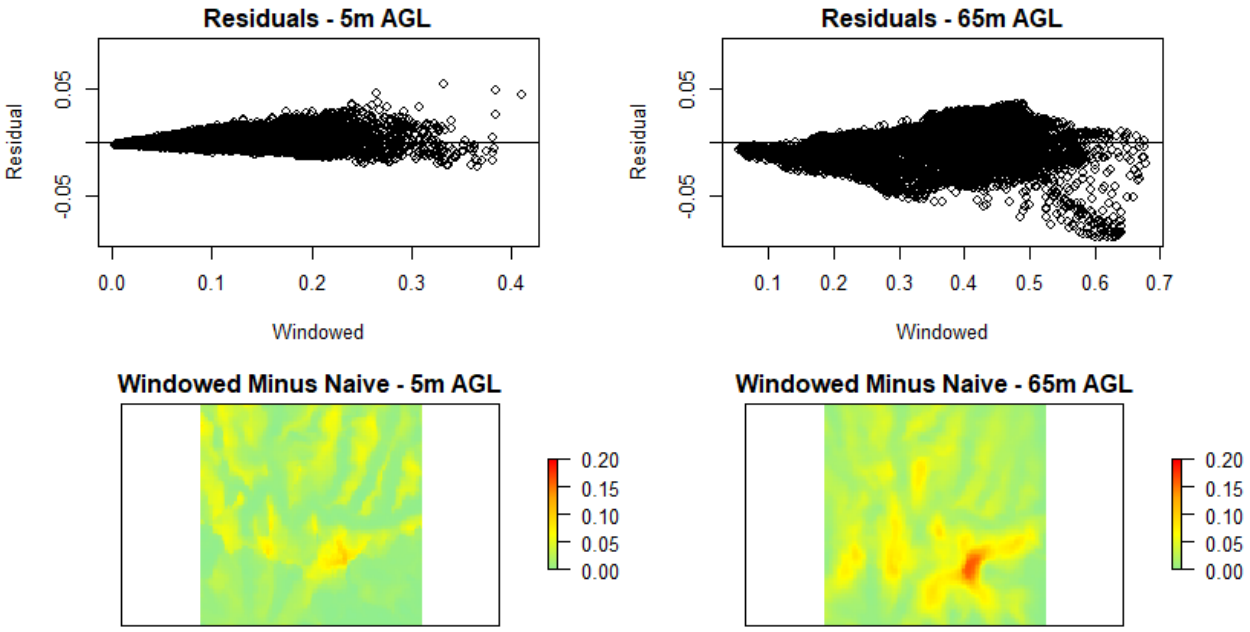

Figure 12: Residual plots for linear models predicting the windowed measure and corresponding plots showing the difference between the two metrics.

As discussed by Ray in his visibility study of the ground layer, higher elevations do not necessarily correspond to higher visibility. This conclusion transfers well to the aerial layer, which can be seen in Figure 13 [10]. An intuitive way to reduce visibility is to 'remain in the low ground,' and this would result in generally lower exposure. However, operational requirements may not permit avoiding transition over higher elevations, and variability at these altitudes provides opportunity to leverage the exposure metric to minimize visibility. The naive metric now appears to be a less suitable substitute for the windowed metric for some applications as it does not as accurately predict values when exposure is highest. An experienced human may be able to rapidly identify areas of moderate to high elevation with minimal exposure, but

autonomous navigation or concealment required for simulations and future systems may leverage the exposure metric to perform the same task.

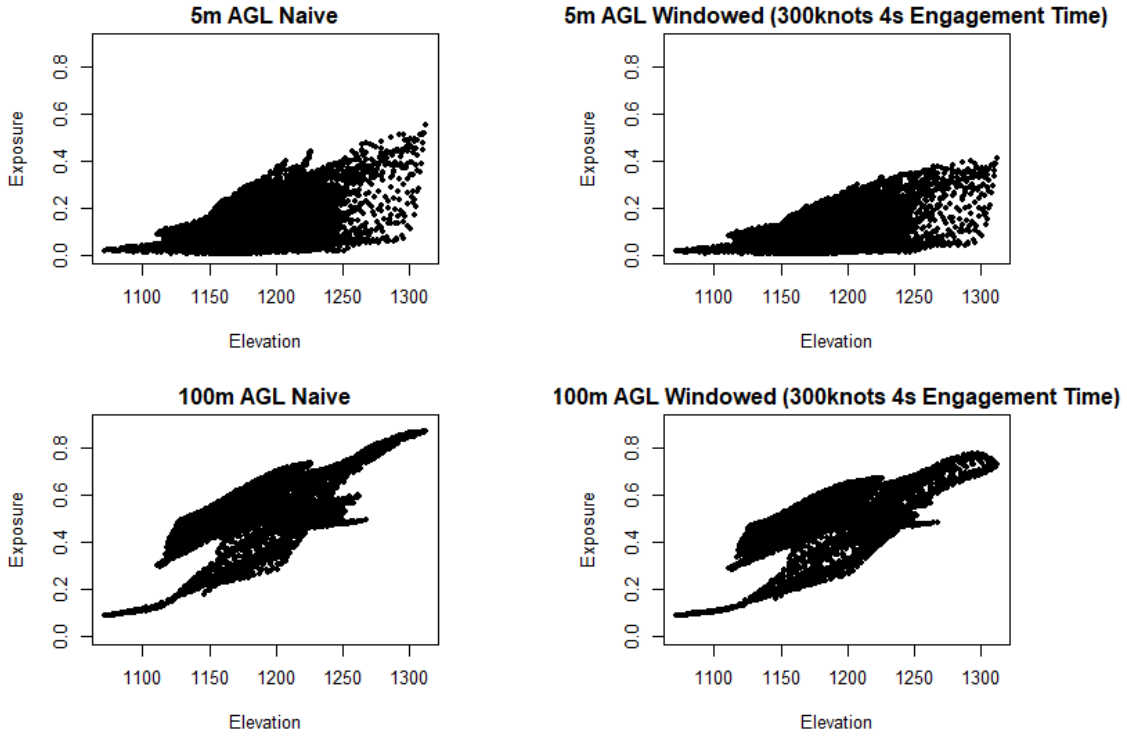

Figure 13: Plots depicting the relationship between exposure and elevation with exposure plotted on the y axes with elevation on the x axes (windowed and naïve).

3.3. COMPUTATIONAL AND STORAGE REQUIREMENTS

Calculating exposure is computational expensive, and requires extremely large data storage capacities for DEM sizes relevant to upcoming studies. Table 2 shows processing and storage requirements for intervisibility at the 3x3 km and 9x27 km terrains calculated at 30m resolution and estimated requirements for larger terrains. Storage and computational requirements both scale logarithmically as the number of elevation postings increase in a DEM. Here, each elevation posting contains information about visibility to every other elevation posting.

Storage Requirements & Computation Times non-Range Limited Intervisibility			
DataSet	**Resolution**	**Storage (Tb)**	**Compute Time**
3x3k	30	.0004	11 Min.
9x27k	30	.29	~19.5 Hours
50x100k	30	123.48	~12 Days
95x126k	50	91.69	~24 Days
100x100k	5	640000	TBD
100x100k	30	493.62	~33 Days
100x100k	50	64	~12 Days

Table 2: Storage Requirements and Compute Times

We can reduce the storage requirements for intervisibility by only storing visibility results within a certain range to each viewpoint. This method may actually be a more useful measure of exposure because air defense system ranges themselves are limited. Furthermore, in larger terrains there may be significant 'edge effects' when considering the entire terrain. Intervisibility from corner to corner is far more likely to be obstructed than intervisibility from center to corner. The estimated storage and computational requirements for range limited intervisibility calculations are shown in Table 3.

Storage Requirements & Computation Times With Max-Range Consideration of **50 km.**			
DataSet	**Resolution**	**Storage (Tb)**	**Compute Time**
50x100k	30	61.73	~9 Days
95x126k	50	19.152	~18 Days
100x100k	5	160000	TBD
100x100k	30	123.4321	~28 Days
100x100k	50	16	~11 Days

Table 3: Computational and Data Storage Requirements for Intervisibility Calculation with Limited Range Consideration of 50km.

3.4. RANGE LIMITED EXPOSURE

In order to compare the results of range-limited exposure we calculated exposure at the levels above in Table 1 for the 3x3 km terrain, but with range limited to 1 km for exposure calculations. The results shown in Figure 14 illustrate a similar pattern to results above without the range limitation. Altitude remains the most significant factor influence exposure, and both airspeed and engagement time have a slightly larger average effect on exposure's overall

magnitude. Exposure at 300m altitude approaches 1 due to the high angle to the 1 kilometer radius surface below the viewpoint.

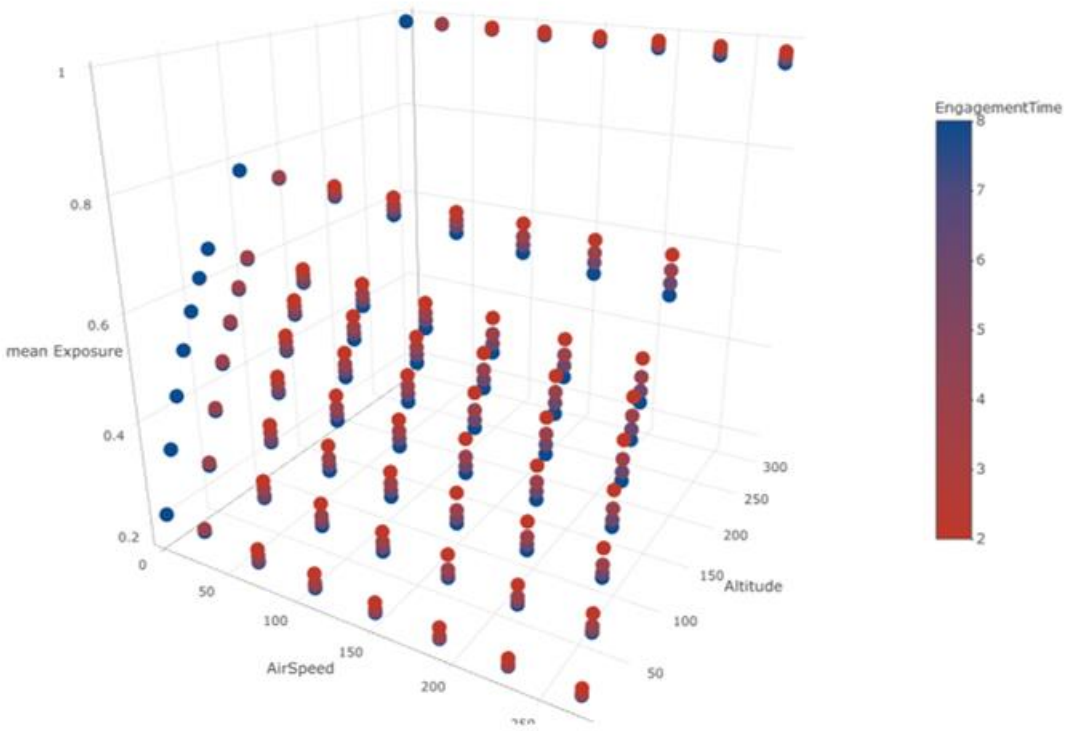

Figure 14: Three-dimensional scatterplot depicting the relationship between: 1-exposure, on the vertical axis, 2-airspeed and altitude, on the horizontal axes, and 3. engagement time, represented by marker color (1 km range limit on 3x3 DEM)

Figure 15 displays exposure surfaces at 4m AGL alongside the original DEM. When compared to the original surface, we note some considerable differences. Firstly, exposure does not correlate with elevation closely as in the original plot. There also appears to be extreme values in corners of the plot where exposure is very high or low. These are likely associated with the limited surface assessed for visibility due to its location in the corner of the DEM.

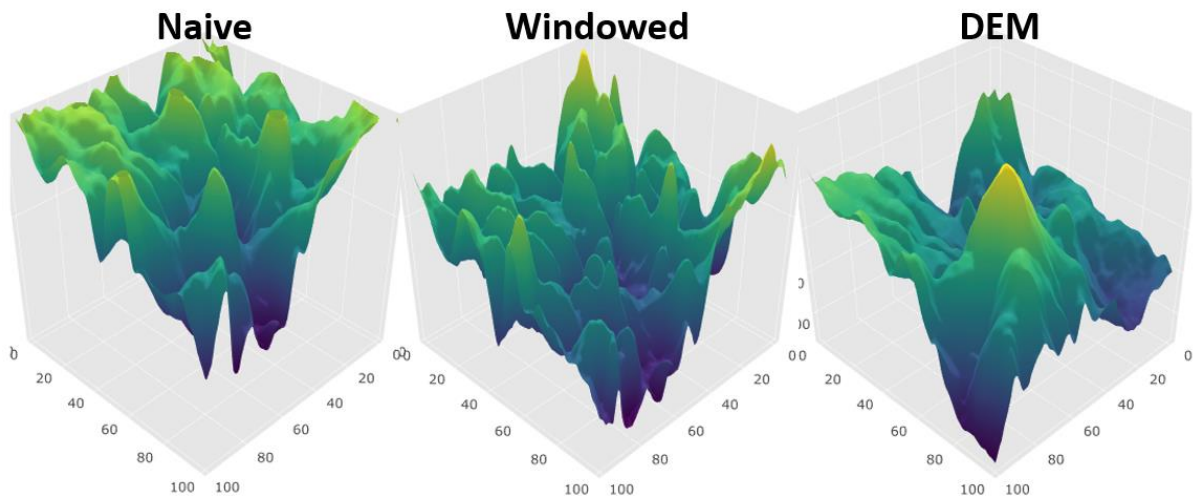

Figure 15: Surfaces depicting range limited & windowed exposure at 270 knots & 5m AGL with 4 second engagement time.

We see a similar result at 65m AGL, with some more evidence of feature alignment with the terrain. This result is shown in Figure 16. In this case, we also see far higher exposure values than in the unlimited range case. The variability associated with range-limited exposure requires that more research be conducted at larger terrain sizes. The relatively small sampling space of the 3x3k DEM does not likely provide the measurement space to determine the utility of a range limited sample.

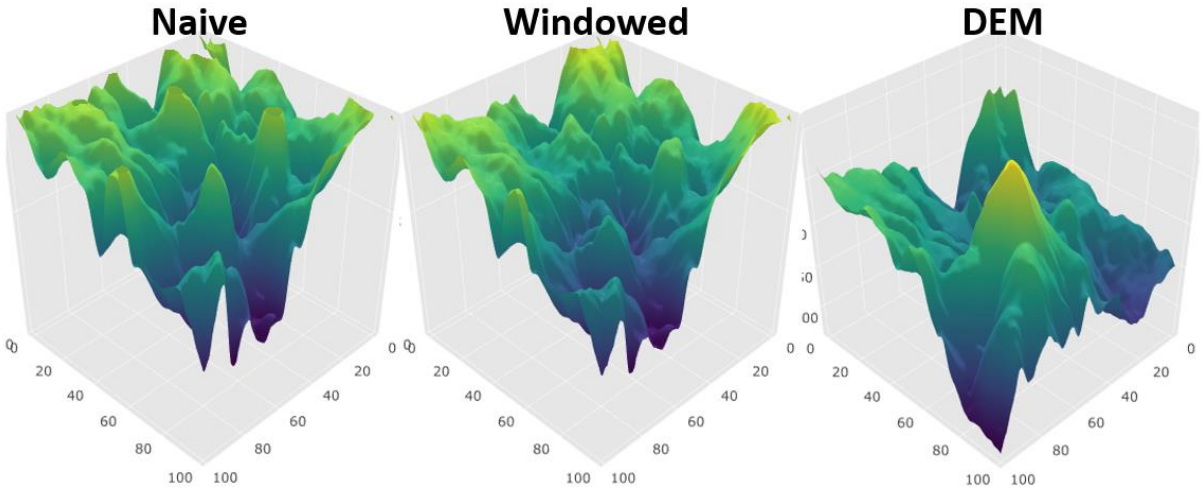

Figure 16: Surfaces depicting range limited & windowed exposure at 270 knots & 65m AGL with 4 second engagement time.

3.5. APPLICATIONS

In this section we provide example applications of the use of the exposure metric to inform the selection of a route with the least cumulative exposure and in the selection of sites for air defense assets.

3.5.2 AERIAL ROUTING

The aerial routing application leveraged the r package gdistance to generate routes for network of nodes where each arc is assigned a cost weighting based on exposure. We construct a single layer network consisting of a node at every elevation posting, each node is connected to all adjacent nodes resulting in eight possible directions of motion. In this construct, routes that minimize cost, exposure in this case, are then determined at a single constant altitude AGL [11]. The 'gdistance' package uses Dijkstra's algorithm to find the least cost (exposure) route,an example of a least cost route is shown in Figure 17 [12]. The route generated follows a reasonable trace through the exposure surface resulting in a path that leverages terrain features to reduce visibility.

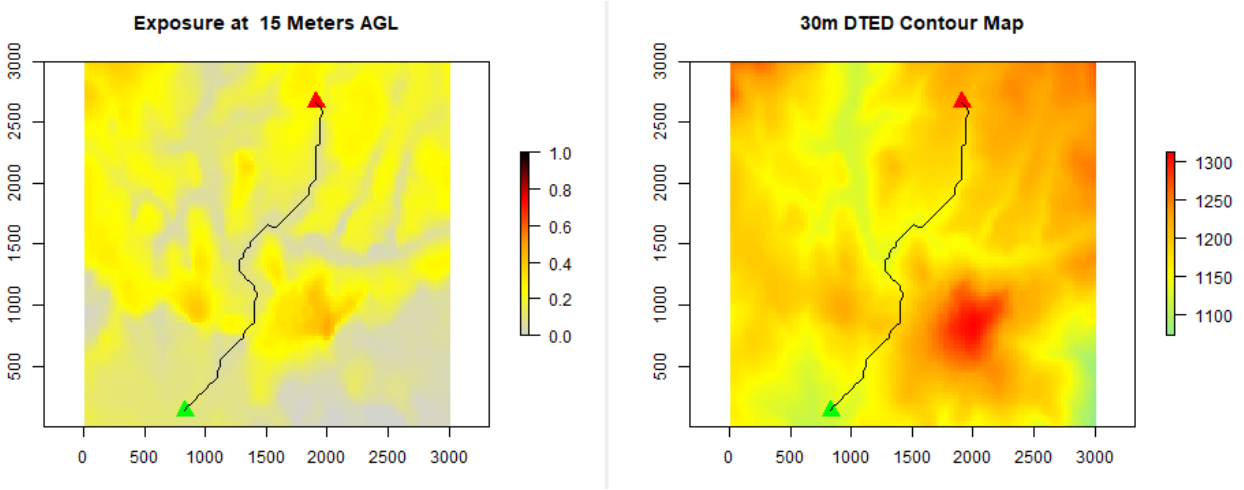

Figure 17: Route that minimize exposure at 15 meters AGL across 3x3 km DEM. Route calculated using Dijkstra's algorithm with each arc assigned a cost weighting based on windowed exposure calculated at 270 knots with a 4 second engagement time.

3.5.2 AIR DEFENSE EMPLACMENT

The second proof of principle application leveraged both exposure and intervisbility data to identify optimal ADA sites within the 3x3 km terrain. The algorithm used a greedy search to maximize the number of points on the map 'covered' or visible by a set of ADA systems. The greedy search identifies the first site as the elevation posting with the highest range limited

section score at a given altitude, and then records which locations are covered by that site. Subsequent sites are determined by maximizing exposure to points not already covered. Figure 18 illustrates results conducted on the 3x3 km terrain with a 1 km range limit with coverage maximized at 15m AGL. As in the routing application, the solution appears reasonable and with further testing could prove useful in simulations or real world applications.

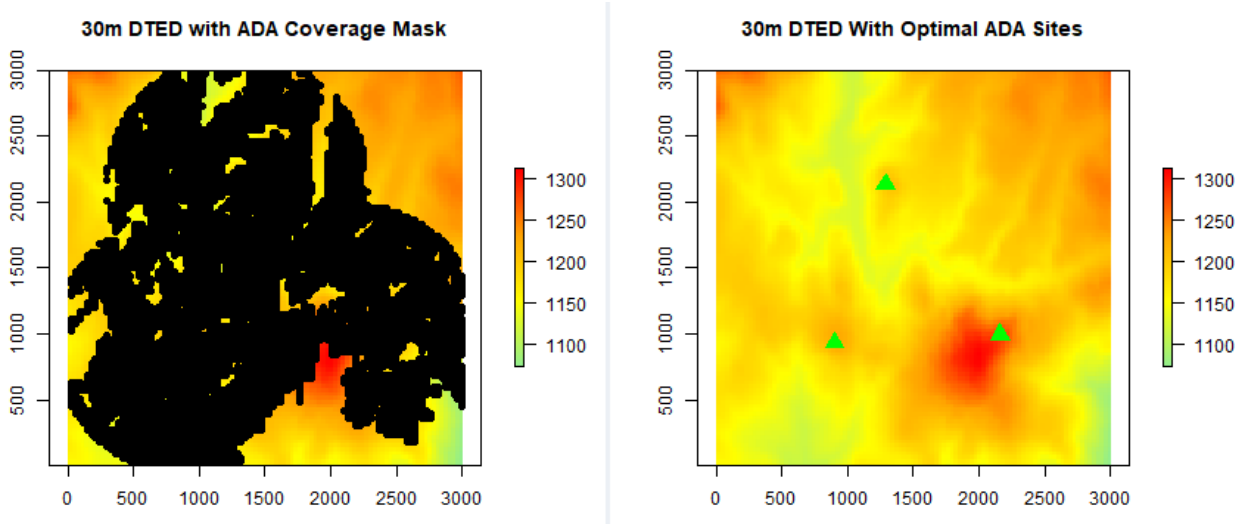

Figure 18: Optimal ADA placement sites based on greedy maximal coverage search. In this example the range of the ADA sites are 1 kmm and coverage is maximize for aircraft at 15m AGL.

SECTION 4. CONCLUSION

We developed of two aerial exposure metric that captures the level of exposure of a point in the air to points on the ground. The metrics possess the potential to inform future studies in support of the acquisition process and provided initial insights on the relationship between aircraft flight profiles and exposure. The geometric intervisibility calculation results in an exposure score that is strongly related to altitude. Incorporating a continuous visibility requirement to a moving aircraft within currently feasible rotary wing speeds did not appear to have an operationally relevant effect on exposure, although more testing is required to confirm this on larger terrains. The calculation of the exposure metric presented was computationally intensive, but provides a basis for testing future models of exposure with lower fidelity. Although the current formulation requires high volume storage and which creates challenges for use, numerous approaches can be taken to reduce these requirements with a baseline understanding of exposure.

Future research on both formulation and applications of the exposure metric is required to enable support to studies and or operational requirements. Reducing storage and computational requirements will enable support in terrain sizes sufficient to support upcoming studies. Examples of potential storage reduction modifications include reductions of terrain resolution, radial rather than coordinate based visibility data storage and calculation, efficient data calculation and storage as presented by Tabik et. al, or a quadtree storage approach. A more complete study of exposure's relationship to an aircraft's flight profile, may reveal flight tactics or aircraft requirements to reduce exposure. Recommendations on overall tactics and requirements may vary for different terrain types, enemy capabilities, or terrain types. Least exposure routing has many opportunities for future research, and initial efforts should focus on incorporating multiple altitudes and airspeeds to provide a complete flight path. The air defense emplacement alogorithm can be improved to account for true system capabilities and techniques that enable successful engagement of targets.

REFERENCES

[1] *FM 3-04.203, Fundamentals of Flight,* Headquarters, Department of the Army, 2007.

[2] *JP 2-01.3,Joint Intelligence Preparation of the Operational Environment,* 2014.

[3] S. Tabik, E. L. Zapata and L. F. Romero, "Simultaneous computation of total viewshed on large high resolution grids," *International Journal of Geographical Information Science,* vol. 27, pp. 804-814, 2013.

[4] H. Haverkort, L. Toma and Y. Zhuang, "Computing Visibility on Terrains in External Memory," *J. Exp. Algorithmics,* vol. 13, 2 2009.

[5] S. Tabik, A. R. Cervilla, E. Zapata and L. F. Romero, "Efficient Data Structure and Highly Scalable Algorithm for Total-Viewshed Computation," *IEEE Journal of Selected Topics in Applied Earth Observations and Remote Sensing,* vol. 8, pp. 304-310, 1 2015.

[6] E. Pfister-Altschul, *Comparison of Ground-to-Air Visibility Analysis Methods*, 2014.

[7] *ArcGIS Pro Visibility Function Manual,* 2017.

[8] M. Llobera, "Extending GIS-based visual analysis: the concept of visualscapes," *International Journal of Geographical Information Science,* vol. 17, pp. 25-48, 2003.

[9] L. Toma, Y. Zhuang, W. Richard and M. Metz, *Viewshed Function Manual,* 2017.

[10] W. R. Franklin and C. K. Ray, "Higher isn't Necessarily Better: Visibility Algorithms and Experiments," *Advances in GIS Research: Sixth International Symposium on Spatial Data Handling,* pp. 751-770, 1994.

[11] J. Etten, "R Package gdistance: Distances and Routes on Geographical Grids," *Journal of Statistical Software,* vol. 76, pp. 1-21, 2017.

[12] E. W. Dijkstra, "A note on two problems in connexion with graphs.," *Numerische Mathematik,* vol. 1, pp. 269-271, 1959.